

Scintillation Detector Spectroscopy

Elijan Mastnak

Winter Semester 2020-2021

Contents

1	Tasks	2
2	Equipment and Procedure	2
2.1	Equipment	2
2.2	Sketch of Procedure	2
2.3	Data	2
3	Analysis	3
3.1	Single-Channel Analyzer	3
3.2	Multi-Channel Analyzer	4
3.3	Cesium Spectrum	5
3.4	Resolutions	5
3.5	Photon Absorption Efficiency	6
4	Error Analysis	7
4.1	Line Energies with Single-Channel Analyzer	7
4.2	Line Energies with Multi-Channel Analyzer	7
4.3	Energy Resolution	7
4.4	Photon Absorption Efficiency	8
5	Results	8
A	Theory	9
A.1	Sodium, Cesium and Cobalt Decay	9
A.2	Gamma Ray Interaction with Crystal	9
A.3	How the Detector Works	10

1 Tasks

1. With both the single and multi-channel analyzers, calibrate the scintillation spectrometer using the ^{22}Na source, then measure the spectra and gamma ray energies of the ^{137}Cs and ^{60}Co sources.
2. Identify the photopeak, Compton peak, and back-scattering peak in the ^{137}Ce spectrum. Estimate the energy of the back-scattering peak.
3. Measure the energy resolution of the photopeak for all three sources. Qualitatively discuss how the resolution changes with energy.
4. Estimate the NaI(Tl) crystal's photon absorption efficiency in the ^{137}Ce photopeak.

2 Equipment and Procedure

2.1 Equipment

1. A scintillation detector, consisting of a NaI(Tl) crystal, photomultiplier, and pre-amplification units. Used to convert gamma decays into measurable current pulses. CAEN N471 high-voltage power supply for the photomultiplier.
2. Single-channel and multi-channel analyzers to measure the gamma ray spectrum.
3. ^{22}Na , ^{137}Cs and ^{60}Co gamma ray sources.

2.2 Sketch of Procedure

1. Connect all elements to their power supplies. Place the ^{22}Na source on scintillator and observe the gamma ray current pulses on the oscilloscope.
2. For each source, use the single-channel analyzer to measure the dependence of pulse counts on the photomultiplier's lower level.
3. Use the multi-channel analyzer to measure the background spectrum. Then use the MCA to measure each source's spectrum. In raw form, the spectrum is counts as a function of channel number.

2.3 Data

Part 1 (SCA): Independent variables are the SCA's lower level and window size (in volts) and measurement time. Dependent variable is the number of gamma ray counts in a given SCA window over a given measurement time.

Part 2 (MCA): Independent variables are channel number and measurement time. Dependent variable is gamma ray counts per channel over a given measurement time.

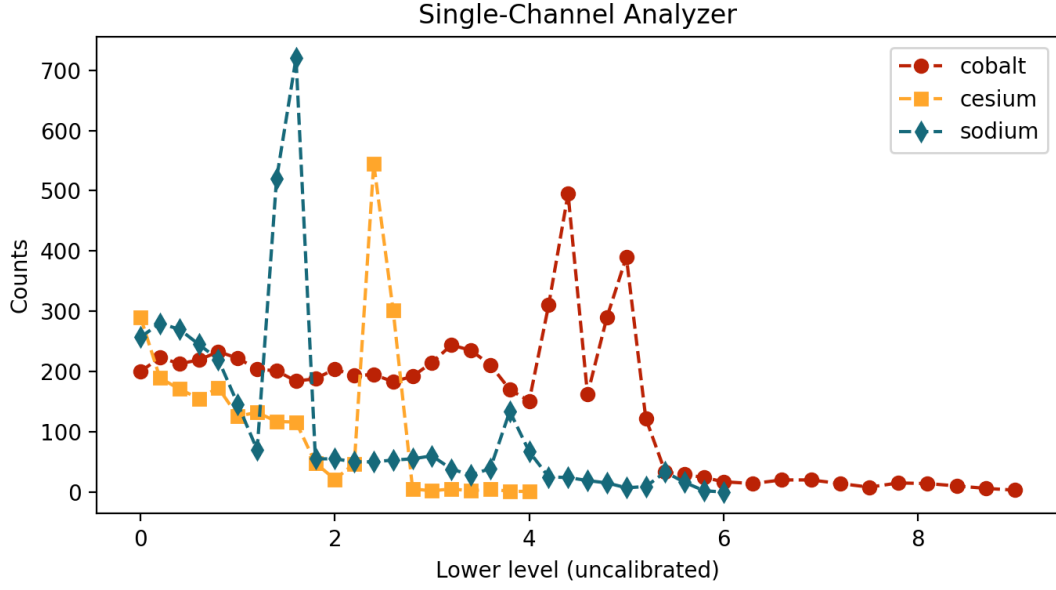


Figure 1: The spectrum of each source measured with the single-channel analyzer. Note the very coarse measurements—see Figure 2 for a higher-quality measurement using a multi-channel analyzer.

3 Analysis

3.1 Single-Channel Analyzer

Using the SCA ^{22}Na data, I identified the SCA lower level numbers n_1 and n_2 corresponding to the $E_1 = 0.51$ MeV and $E_2 = 1.277$ MeV peak, and then interpolated a linear $E(n)$ characteristic with

$$E(n) = E_1 + \left(\frac{E_2 - E_1}{n_2 - n_1} \right) (n - n_1)$$

I then estimated the energies of the ^{137}Cs and ^{60}Co peaks using the $E(n)$ equation. Table 1 shows the results.

Isotope	Lower Level [V]	Energy Estimate [MeV]	True Energy [MeV]
^{22}Na	1.6 ± 0.2	-	0.511
^{22}Na	3.8 ± 0.2	-	1.277
^{137}Cs	2.4 ± 0.2	0.80 ± 0.38	0.667
^{90}Co	4.4 ± 0.2	1.48 ± 0.17	1.173
^{90}Co	5.0 ± 0.2	1.68 ± 0.16	1.332

Table 1: Rough estimates of spectral line energies using the single-channel analyzer.

Note: If I remember correctly, I slightly adjusted the photomultiplier’s amplification setting when switching to the cobalt source, which explains the systematically too-large energy estimate for the cobalt peaks.

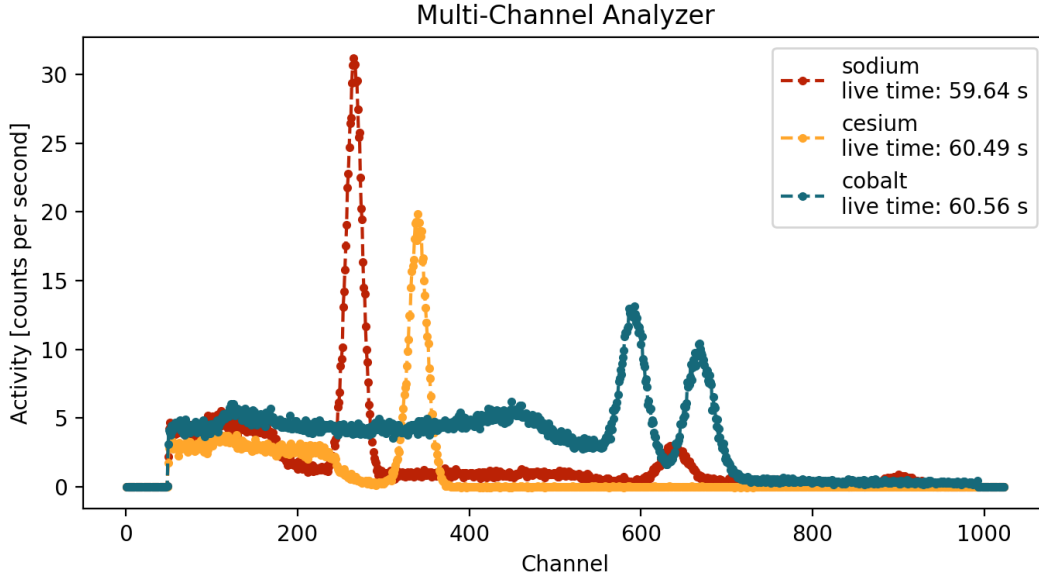


Figure 2: The spectrum of each source measured with the multi-channel analyzer.

3.2 Multi-Channel Analyzer

To account for different samples (in particularly the background) being measured for different times, I first converted count data to activity by dividing counts by measurement time.

$$A = \frac{N}{t_{\text{live}}}$$

I then subtracted the background spectrum from the sodium, cobalt, and cesium data. I then repeated the calibration procedure from channel number to energy using the known values of the two sodium spectral lines.

$$E(n) = E_1 + \left(\frac{E_2 - E_1}{n_2 - n_1} \right) (n - n_1)$$

With this relationship, I found the energy E of the main spectral lines using the known channel number n . Table 2 shows the results.

Isotope	Channel	Energy Estimate [MeV]	True Value [MeV]
^{22}Na	264 ± 1	-	0.511
^{22}Na	636 ± 1	-	1.277
^{137}Cs	339 ± 1	0.665 ± 0.021	0.667
^{60}Co	589 ± 1	1.180 ± 0.006	1.173
^{60}Co	667 ± 1	1.341 ± 0.006	1.332

Table 2: Estimates of spectral line energies using the multi-channel analyzer.

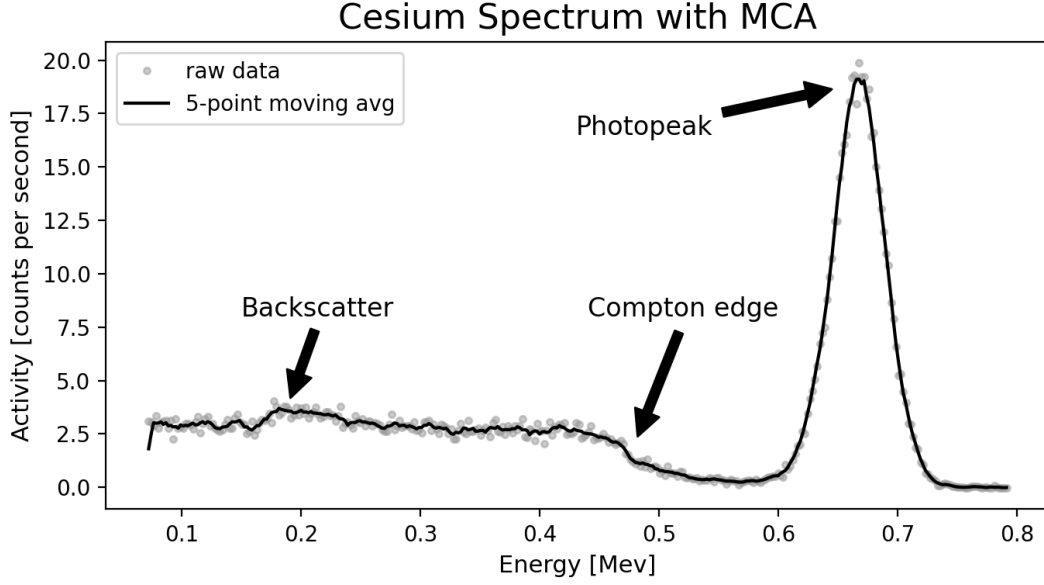


Figure 3: Prominent components of the ^{137}Ce spectrum with energy calibrated as described in Subsection 3.2.

3.3 Cesium Spectrum

Figure 3 identifies the ^{137}Ce backscatter peak, Compton edge, and photopeak.. I used a 5-point moving average to help estimate the corresponding energies as:

Backscatter peak:	$(0.18 \pm 0.01) \text{ MeV}$
Compton edge:	$(0.47 \pm 0.01) \text{ MeV}$
Photopeak:	$(0.667 \pm 0.003) \text{ MeV}$

Note that the backscatter peak's energy is roughly the photopeak energy minus the energy of the Compton edge. The uncertainties on the backscatter and Compton energies are rough visual estimates—the photopeak uncertainty is separation between neighboring points.

3.4 Resolutions

I fit a Gauss curve to each photopeak peak to find the peaks standard deviation σ , found the FWHM with $\text{FWHM} \approx 2.355\sigma$, then found the peak's resolution R with

$$R = \frac{\Delta E}{E}$$

where E is the peak's energy and ΔE is the FWHM. Note that resolution decreases (improves) with increasing energy. This is expected—from the Poisson statistics of light production in the scintillator we have $\Delta E \propto E$ and thus $R \propto \frac{1}{\sqrt{E}}$. In other words, the observed decrease in R with respect to E agrees with theory.

Isotope	Line Energy [MeV]	FWHM [MeV]	Resolution
^{22}Na	0.511 ± 0.001	0.047 ± 0.000	0.092 ± 0.001
^{137}Cs	0.665 ± 0.021	0.052 ± 0.000	0.078 ± 0.003
^{60}Co	1.180 ± 0.006	0.083 ± 0.001	0.071 ± 0.001
^{60}Co	1.341 ± 0.006	0.084 ± 0.001	0.062 ± 0.001

Table 3: Resolution of spectral lines. The uncertainty in sodium is relatively low because of the low uncertainty in line energy—we assumed the known value 0.511 MeV *a priori*. To three decimal places, the uncertainty in FWHM, estimated from the covariance matrix returned by SciPy’s `curve_fit`, is essentially zero.

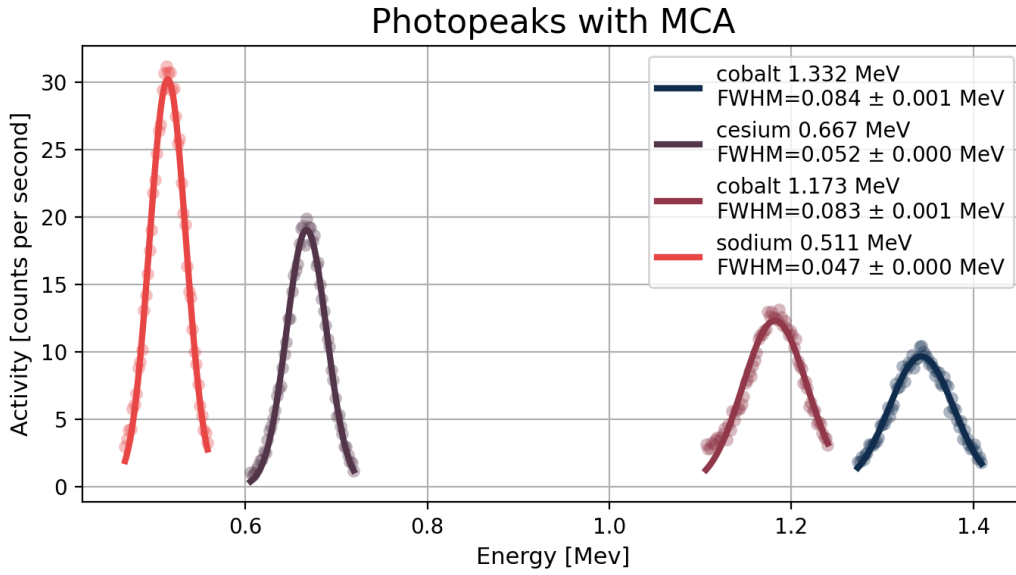


Figure 4: Full-width at half maximum of each photopeak. The analysis is performed by fitting a Gauss curve to each photopeak using SciPy’s `curve_fit`.

3.5 Photon Absorption Efficiency

I estimated the NaI crystal’s photon absorption efficiency with the ^{137}Cs source as

$$\eta = \frac{N_{\text{peak}}}{N_{\text{all}}} = \frac{A_{\text{peak}}}{A_{\text{all}}}$$

where N_{peak} is the number of pulses registered in the photopeak and N_{all} is total number of gamma rays in the solid angle 2π , and the A values are the corresponding activities. I was given the source’s half-life and January 2013 activity: 30.7 years and 9250 Bq, respectively. I estimated the October 2020 activity using the radioactive decay law

$$A(t) = A_0 e^{-t/\tau} \implies A_{2020} = A_{2013} \exp\left(-\ln 2 \cdot \frac{7.83 \text{ years}}{30.7 \text{ years}}\right) = 7750 \text{ Bq}$$

A_{2020} represents isotropic activity over the entire solid angle 4π (not 2π), so I divided A_{2020} by a factor of 2, and then multiplied A_{2020} by 0.946, since the rate of ^{137}Cs

0.667 MeV emission is 0.946 times the source activity (see Appendix A.1). From Figure 3, we see activity at the cesium photopeak is about $A_{Cs} = 19.5 \text{ Bq}$. The crystal's efficiency is thus

$$\eta = \frac{N_{\text{peak}}}{N_{\text{all}}} = 2 \cdot \frac{A_{Cs}}{0.946 \cdot A_{2020}} = 2 \cdot \frac{19.5 \text{ Bq}}{0.946 \cdot 7750 \text{ Bq}} \approx 0.0053$$

4 Error Analysis

4.1 Line Energies with Single-Channel Analyzer

Input data is lower level n and the known ^{22}Na energies E_1 and E_2 . I estimated the lower-level position error as $u_n = 0.2 \text{ V}$, the separation between points and took $E_{1,2}$ to have zero uncertainty. I modified the interpolation formula as follows

$$E(n) = E_1 + \left(\frac{E_2 - E_1}{n_2 - n_1} \right) (n - n_1) \equiv E(n) = E_1 + \frac{E_2 - E_1}{\Delta n_1} \Delta n_2$$

where I introduce the two lower-level differences Δn_1 and Δn_2 as input quantities, each with error $u_{1,2} = 2 \cdot 0.2 \text{ V} = 0.4 \text{ V}$, since error adds under subtraction. The sensitivity coefficients are

$$c_1 = \frac{\partial E}{\partial \Delta n_1} = -\Delta n_2 \frac{E_2 - E_1}{\Delta n_1^2} \quad \text{and} \quad c_2 = \frac{\partial E}{\partial \Delta n_2} = \frac{E_2 - E_1}{\Delta n_1}$$

while the error on the energy estimate E is

$$u_E = \sqrt{(u_1 c_1)^2 + (u_2 c_2)^2}$$

Table 1 shows the results. This analysis assumes, perhaps too liberally, a simple linear relationship between E and n .

4.2 Line Energies with Multi-Channel Analyzer

Since I used the same linear interpolation procedure to find the line energies with the MCA as with the SCA, the corresponding error analysis for the MCA is completely analogous the above approach for the PCA. I simply replaced the role of the SCA lower level with MCA channel number, which I took to have an uncertainty of $u_c \pm 1$ at the peak positions. Table 2 shows the results.

4.3 Energy Resolution

Input quantities are line energy E and peak FWHM ΔE . Table 2 shows the error in line energies u_E . I estimated error in FWHM $u_{\Delta E}$ as the square root of the corresponding element in the covariance matrix returned by `curve_fit` when fitting a bell curve to the peak.

$$R = \frac{\Delta E}{E}$$

Sensitivity coefficients are

$$c_{\Delta E} = \frac{\partial R}{\partial \Delta E} = \frac{1}{E} \quad \text{and} \quad c_E = \frac{\partial R}{\partial E} = -\frac{\Delta E}{E^2}$$

The associated error is

$$u_R = \sqrt{(u_{\Delta E} c_{\Delta E})^2 + (u_E c_E)^2}$$

4.4 Photon Absorption Efficiency

I did not calculate error on the estimated efficiency, since the efficiency value is intended more as an order of magnitude estimate than an exact result. Additionally, the two input quantities, half-life and initial activity, are given without any uncertainty. I would have to “invent” uncertainties in these two quantities if I were to calculate error in efficiency, which would then be somewhat arbitrary anyway.

5 Results

The estimates of the photopeak energies using the single channel analyzer, shown in Table 1 and reprinted below, were poor. As discussed in the analysis, I believe the values for cobalt are additionally skewed by my having tinkered with the photomultiplier’s amplification settings without re-calibrating the scintillation detector.

Isotope	Energy Estimate [MeV]	True Energy [MeV]
^{137}Cs	0.80 ± 0.38	0.667
^{90}Co	1.48 ± 0.17	1.173
^{90}Co	1.68 ± 0.16	1.332

Table 4: Rough estimates of spectral line energies using the single-channel analyzer.

The estimates of the photopeak energy using the multi-channel analyzer are much closer to the true values. The results, from Table 1, are re-printed below:

Isotope	Energy Estimate [MeV]	True Energy [MeV]
^{137}Cs	0.665 ± 0.021	0.667
^{60}Co	1.180 ± 0.006	1.173
^{60}Co	1.341 ± 0.006	1.332

Table 5: Estimates of spectral line energies using the multi-channel analyzer.

The sources’ photopeak resolutions ranged from about 5 to 10 percent. As theoretically expected, resolution improved with increasing photopeak energy. The results are below:

Isotope	Line Energy [MeV]	Resolution
^{22}Na	0.511 ± 0.001	0.092 ± 0.001
^{137}Cs	0.665 ± 0.021	0.078 ± 0.003
^{60}Co	1.180 ± 0.006	0.071 ± 0.001
^{60}Co	1.341 ± 0.006	0.062 ± 0.001

Table 6: Resolution of spectral lines. Uncertainty in ^{22}Na is relatively low because the line energy of 0.511 MeV was assumed with low uncertainty *a priori*.

The crystal's efficiency for photon absorption, estimated using the photon activity registered in the ^{137}Cs photopeak, was roughly $\eta \approx 0.005$.

A Theory

The experiment's goal is to measure the energy of gamma rays. This done indirectly by measuring the energy of photons created by the gamma rays e.g. in our case with a scintillation detector.

A.1 Sodium, Cesium and Cobalt Decay

- Sodium scheme: ^{22}Na has a 90.2 percent probability for β^+ decay and a 9.7 percent probability for electron capture into an excited state of ^{22}Ne . Nearly 100 percent of the time, the neon nucleus decays to the ground state by emitting a 1.27 MeV photon. Meanwhile, the positron from beta decay annihilates with a surrounding electron and produces two 0.511 MeV gamma rays.

The rates of 1.27 MeV and 0.511 MeV gamma ray emission are equal to the source activity and $(2 \cdot 0.9 = 1.8)$ times the source activity, respectively.

- Cesium: ^{137}Cs has a 5.4 percent chance to decay directly into the ^{137}Ba ground state via β^- decay and a 94.6 percent probability for β^- decay into an excited ^{137}Ba nucleus, which then decays to the ^{137}Ba ground state by emission of a 0.667 MeV photon. The rate of 0.667 MeV gamma emission is thus 0.946 times the source activity.
- Cobalt: ^{60}Co decays by β^- emission to an excited ^{60}Ni state 2.507 MeV above the ground state. This excited state decays by emission of a 1.175 MeV gamma ray, followed within a picosecond or so by a 1.332 MeV gamma ray. The rate of emission for both gamma rays approximately equals the source activity.

A.2 Gamma Ray Interaction with Crystal

- Photoelectric effect: incident gamma ray gives up its energy to eject a bound inner shell electron (binding energy of order 10 keV) from one of the scintillator crystal's atoms. All gamma ray energy is deposited into scintillator. Corresponds to the *photopeak*.
- Compton effect: when gamma rays first strike the lead shield and then Compton scatter back into the scintillator at reduced energy. Corresponds to the low-energy *back-scatter peak*.

Compton plateau: corresponds to gamma rays Compton scattering off atoms in the scintillator crystal. The recoiling electron's energy is deposited in the crystal, while the scattered gamma photon exits the crystal undetected.

The electron's recoil energy depends on the angle of the scattered photon. Recoil energy varies from a maximum when the photon back-scatters (corresponding to the *Compton edge*), to zero when the photon is scattered in the forward direction.

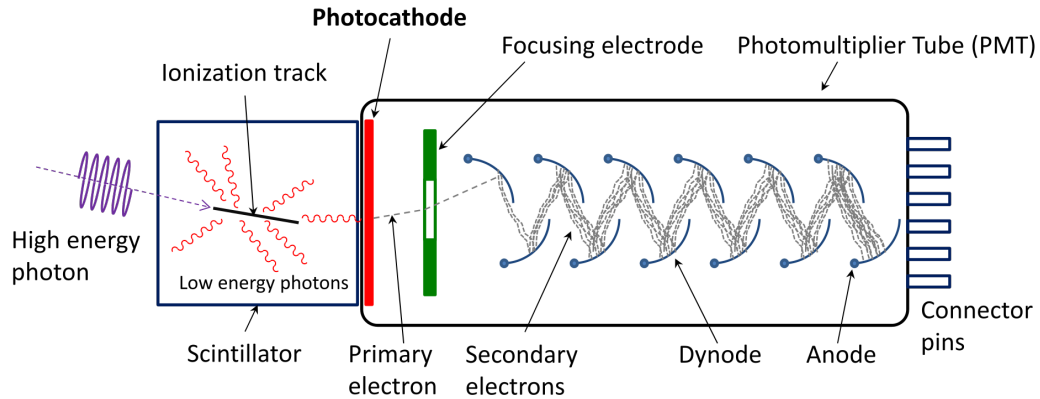


Figure 5: Schematic of a scintillation detector (from Wikipedia)

- Pair production: In the strong electric fields near scintillator crystal nuclei, a gamma ray can create an electron-positron pair as long as the gamma ray energy exceed the 1.022 MeV rest mass energy of an electron-positron pair. Gamma energy in excess of 1.022 MeV contributes to the kinetic energy of the electron and positron; the extra kinetic energy is quickly absorbed in the crystal.

When the positron gets to low enough energy, it annihilates with an electron in the crystal, which produces two 0.511 MeV annihilation gamma rays.

If both annihilation gamma rays are absorbed in the crystal, the total absorbed energy is the original gamma energy, and the event contributes to the *photopeak*.

If one or both of the annihilation gamma rays escape from the crystal, the event registers in one of two small peaks (either the *single* or *double escape peak*) that are either 0.511 MeV or 1.022 MeV below the photopeak.

Quick Review of Photoelectric Effect and Compton

- Photoelectric effect: Photons incident on material eject electrons.
- Compton scattering: scattering of photons by a charged particle with an accompanying wavelength shift for the scattered photon.
- Pair production: production of a particle and antiparticle from a neutral boson, in our case electron-positron production from a photon.

A.3 How the Detector Works

- Gamma ray from the radioactive source pass through the NaI crystal. The gamma rays interact with the crystal and create scintillation photons (in the visible and ultraviolet spectrum).
- The scintillation photons strike the photomultiplier's cathode and eject electrons via the photoelectric effect. The electrons emitted from the cathode are

accelerated by a high voltage through a dynode chain before reaching a collector anode. The dynodes serve as electron multipliers, and the entire dynode chain typically amplifies the electron current by a factor of order 10^6 .

- The anode connects to a series of amplifiers, which convert the collected charge to a proportional voltage pulse. Because the number of scintillation photons produced in the NaI crystal is proportional to the absorbed gamma ray energy, so too are the number of photoelectrons from the cathode, the final anode charge, and the amplitude of the preamp and amplifier voltage pulses. The overall effect is that the final pulse height is proportional to the gamma ray energy absorbed in crystal.